J Radioanal Nucl Chem
DOI 10.1007/s10967-015-4107-4

Trace metal and rare earth elements in a sediment profile from the Rio Grande Reservoir, São Paulo, Brazil: determination of anthropogenic contamination, dating, and sedimentation rates

Robson Leocádio Franklin[1] · Déborah Inês Teixeira Fávaro[2] · Sandra Regina Damatto[3]

Received: 1 December 2014
© Akadémiai Kiadó, Budapest, Hungary 2015

Abstract The Rio Grande Reservoir supplies water to four counties. Two sediment cores were collected, one was sliced every 2 cm for INAA and dating determinations; the other was cut every 5 cm, for grain size and Hg, Cd, Pb, Ni, Mn and Cu determinations. Sedimentation rates and sediment ages of every layer were determined by ^{210}Pb method. Enrichment Factor (EF) and Geoaccumulation Index (I_{geo}) were calculated. Significant enrichment was found for Na, Mn, Ni, Pb, Sb and Zn and extremely high enrichment for Hg, Cu and Cd, in upper layers. A 90 year pollution history of this reservoir was traced.

Keywords Metals and trace elements · Sediment · ^{210}Pb method · Enrichment factor · Geoaccumulation index · Rio Grande Reservoir

Introduction

Sediment compartments have been increasingly used in quality evaluation studies in aquatic ecosystems as they record historic conditions of anthropogenic activity influences, which are not always detectable in water compartments. The interaction between the sediment compartment and the water column can be a source of contamination: the interaction may occur through the revolving sediment because of the increased flow from rainfall or another activity interfering with the dynamics of the riverbed [1]. The sediment, from the recycling of material and energy flow point of view, is one of the most important compartments of aquatic ecosystems. Biological, physical, and/or chemical processes occurring influence the metabolism of the entire system therein, from benthic organisms to ichthyofauna and algae.

Metals of anthropogenic origin, upon entering an aquatic system, can be in their dissolved form (M $(aq)^{+x}$) predominantly and, depending on their characteristics, can remain dissolved or form organic and/or inorganic complexes. This, in turn, may remain in the dissolved state, form colloids or be absorbed by suspended particles in the water body and, then, be deposited in the sediment [2, 3].

One of the major questions in environmental evaluations is how much an ecosystem can be contaminated by a given metal. Many times, the anthropogenic enrichment of a given element could cause great concern even though the high concentration would not result in toxic effects because this metal is in a not readily available form to the biota, either as sulfide or highly complexed organic matter. Another important aspect to take into consideration is to verify if the internationally accepted sediment quality guide values used (for example, PEL, TEL or crust average) are adequate for tropical conditions [4, 5], since they can lead to wrong data interpretation of the metal evaluations in aquatic bodies.

However, when dealing with artificial reservoirs, this issue becomes a complex task, especially in function of their allochthonous characteristics. The sediments of

✉ Sandra Regina Damatto
damatto@ipen.br

[1] Departamento de Análises Ambientais, Companhia Ambiental do Estado de São Paulo (CETESB), Av. Professor Frederico Hermann Jr. 345, São Paulo 05459-900, Brazil

[2] Laboratório de Análise por Ativação Neutrônica (LAN/CRPq), Instituto de Pesquisas Energéticas e Nucleares (IPEN/CNEN - SP), Av. Professor Lineu Prestes 2242, São Paulo 05508-000, Brazil

[3] Laboratório de Radiometria Ambiental (LRA/GMR), Instituto de Pesquisas Energéticas e Nucleares (IPEN/CNEN - SP), Av. Professor Lineu Prestes 2242, São Paulo 05508-000, Brazil

Published online: 02 April 2015

reservoirs or dams operate as true deposits of particulate materials from the rivers that form them. Artificial reservoirs have high sediment rates, when compared to those of the rivers that flow into them, which are lotic systems, while the reservoirs are lentic systems. This difference influences the local sedimentation rates. Furthermore, depending on the location, the alterations that occur in the sediment may be characterized in relatively short periods of time, as little as 5 years or less, in a 10 cm layer of recent sediment. Hence, artificial reservoirs are not very much affected by diagenetic processes and provide preserved historic records, from a lithological point of view, of the metal concentrations in their deeper sediment [6].

Metal evaluations in sediment profiles [5, 6], to obtain the basal levels of the sediments, mainly in tropical reservoirs where temperature dynamics and consequently the weathering are greater [7], are a key point to ascertain whether or not an environment presents anthropogenic contamination or, merely, a lithological enrichment. In order to best establish this difference, both the Enrichment Factor (EF) and the Geoaccumulation Index (I_{geo}) are used [6, 8–10].

The Rio Grande Reservoir was built in the 1920s, is located in the São Paulo Metropolitan Region (RMSP) and covers São Bernardo do Campo, Rio Grande da Serra, Santo André and Ribeirão Pires municipalities, in the state of São Paulo, in Brazil. This reservoir supplies water for around 1.8 million inhabitants. It is, also, used for leisure and recreation by the city's population, and its fish is consumed by inhabitants of the surrounding areas. It is a branch of the Billings Reservoir, and the total area, Billings plus Rio Grande, is 1560 km^2. The Rio Grande reservoir is approximately 10 km long, the maximum distance between margins of 1500 m and provides 4 m^3/s of water for public supply. In 1982, it was separated from the already highly polluted Billings Reservoir in an attempt to preserve its water quality. This separation eliminated the entrance of polluted waters from the city of São Paulo [8].

This reservoir has been studied since 2000 when, in order to evaluate the historical registration of anthropogenic contamination, four sediment cores were sampled. Hg concentration by CV AAS, major and trace elements by INAA and the sedimentation rates by ^{210}Pb method were assessed. The results presented Hg levels much higher than those expected and varying according to depth. The first large Hg discharge occurred at the beginning of the 50's and another one, more severe, during the 80's and 90's. As a general trend, the elemental concentration decreased with depth, indicating recent contamination. The authors suggest further investigation of point 01 (core 01), located near the catchment point of water supply [11].

Bostelman [12], studying this reservoir, also inspected four sampling points located near the sampling points of Favaro et al. study [11]. In another survey [8], bottom sediment samples were collected during dry and rainy seasons, in four different sampling points, located near the sampling points of Bostelman study [12]: INAA assessed metals and trace elements. The results showed the elements As, Br, Sb, Th, U and Zn enriched in relation to the earth crust used as reference value and Sc as normalizer element, mainly at the point that receives domestic and industrial effluents from the rivers that reach the reservoir, opposite to the point of water supply.

In order to continue these studies, the objective of the present study was to evaluate two sediment profiles collected in Rio Grande Reservoir to determine basal values of some trace, metals and rare earth elements, as well as to determine their anthropogenic pollution levels more recently using different analytical techniques, INAA, GFAAS and ICP-OES. The dates and sedimentation rates by ^{210}Pb method were, also, determined in one of the sediment profiles.

Experimental

Sampling and sample preparation for analysis

Two sediment profiles (0.40 and 0.36 m) were collected, in November 2011, in front of the water catchment point of the reservoir for the public water system, coordinates S 23°46′18″and W 46°31′35″, as showed in Fig. 1.

The first sediment profile was sliced every 5 cm, air dried at 20–25 °C in a clean vessel, during approximately 3 days, and separated in two aliquots: one for grain size determination and another for Hg and other metals, by ICP-OES (Inductively Coupled Plasma–Optical Emission Spectrometry) and GFAAS (Graphite Furnace Atomic Absorption Spectrometry). This aliquot was passed through a 2.00 mm sieve, ground in a mortar and, then, homogenized before analysis.

The second sediment profile was sliced every 2 cm, air dried at 20–25 °C in a clean vessel, during approximately 3 days, passed through a 2.00 mm sieve, ground in a mortar, then, homogenized before INAA and dating analysis.

Inaa

Instrumental neutron activation analysis (INAA) has been extensively employed in geochemical studies due to the possibility of quantifying many elements, at the same time, with excellent precision and accuracy and without the need of previous digestion processes. The detection limits varied from 0.01 to 1 mg kg^{-1}, for most elements. About 150 mg of sediment (duplicate samples) and reference materials were accurately weighed and sealed in pre-cleaned

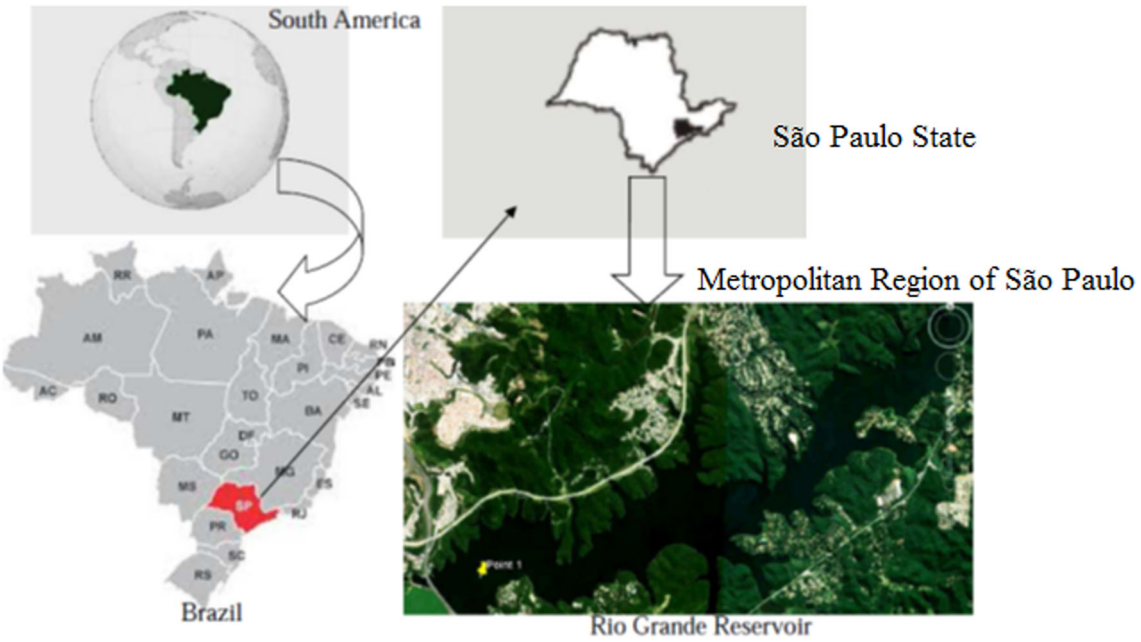

Fig. 1 Sampling point location

polyethylene bags, for irradiation. Sediment samples and reference materials were irradiated for 8 h, under a thermal neutron flux of 1–5 $\times$ 10^{12} n cm^{-2} s^{-1}, at the IEA-R1 nuclear research reactor, at IPEN. Two series of counting were made: the first, after 1 week decay (^{76}As, ^{82}Br, ^{47}Ca, ^{42}K, ^{140}La, ^{24}Na, ^{147}Nd, ^{239}Np, ^{122}Sb, ^{153}Sm and ^{175}Yb were measured) and the second serie, after 15-20 days (^{131}Ba, ^{141}Ce, ^{60}Co, ^{57}Cr, ^{134}Cs,^{152}Eu, ^{59}Fe, ^{181}Hf, ^{177}Lu, ^{233}Pa, ^{86}Rb, ^{124}Sb, ^{46}Sc, ^{182}Ta, ^{160}Tb,^{169}Yb and ^{65}Zn were measured). Gamma spectrometry was performed using a Canberra gamma X hyperpure Ge detector and associated electronics, with a resolution of 0.88 and 1.90 keV for ^{57}Co and ^{60}Co, respectively.

The data analysis was undertaken by using an in-house gamma ray software, VISPECT program to identify the gamma-ray peaks and by ESPECTRO program to calculate the concentrations. Sample and standard counting statistics and sample and standard masses were considered in the uncertainty assessment of the results. The counting statistics component is the most important contribution to the activity uncertainty in INAA [13]. More details of the experimental procedure have already been published by Larizzatti et al. [14]. For methodology validation regarding precision and accuracy, reference materials SL-1 (Lake Sediment—IAEA), BEN-Basalt-IWG-GIT and Soil 5 (IAEA) were used.

^{210}Pb dating methodology

The dates and sedimentation rates were determined by ^{210}Pb method using the measurement of the radionuclides ^{226}Ra and ^{210}Pb in each slice of the profile. The sediment samples, previously dried, grounded and homogenized, were dissolved, 1.00 g, in mineral acids, (HNO_3 conc. and HF 40 %), and H_2O_2 30 % in a microwave digestor, undergoing a radiochemistry procedure to determine Ra and Pb concentrations. This procedure consists in an initial precipitation of Ra and Pb with H_2SO_4 3 M, dissolution of the precipitate with nitrile-tri-acetic acid at basic pH, precipitation of Ba(^{226}Ra)SO_4 with ammonium sulfate and precipitation of $^{210}PbCrO_4$ with sodium chromate 30 %. The ^{226}Ra concentration was determined by gross alpha counting of the precipitate of Ba(^{226}Ra)SO_4, after 21 days of precipitation and the ^{210}Pb concentration through its decay product ^{210}Bi, after 10 days of precipitation, by measuring the gross beta activity of the precipitate of $^{210}PbCrO_4$. The analyzes were performed in duplicate, and both radionuclides were determined in a low background gas flow proportional detector. The detection limits for ^{226}Ra and ^{210}Pb measurements were 2.2 and 4.9 mBq kg^{-1}, respectively [15, 16].

Metals determined by ICP-OES, GFAAS and direct mercury analyzer

The sediment samples were previously digested according to EPA 3051 [17], with HNO_3 and HCl in a microwave oven. The metals Cu, Ni, and Mn were determined by ICP-OES; Cd and Pb, by GFAAS; mercury was determined by Direct Mercury Analyser. These analyzes were performed at the Inorganic Chemistry Laboratory of the Environmental Agency of São Paulo State (CETESB). The analyzes were performed in duplicate. Direct analysis of Hg

has the advantage of exempting the steps of sample preparation, and it is applicable to some matrices. This technique effectively determines the total mercury amounts in the sample and, it also includes determining volatile Hg species, under the conditions of the method.

Three sequential steps comprise this analytical technique, thermal decomposition, in which the sample undergoes a drying process and combustion (approximately 650 °C), under constant flow of oxygen gas (O_2). These combustion products are loaded by O_2 to a catalytic section, which will retain possible interferences in the determination of Hg. In the amalgamation, the remaining gaseous species in the process of thermal decomposition are loaded to an amalgamator. After retention time of Hg vapor, the amalgamator is heated to 850 °C to release the trapped Hg, which volatilizes to be loaded by the O_2 flow to the atomic absorption cell; there, the transient Hg vapor will absorb the radiation from an Hg vapor lamp, emitting a narrow band of wavelengths of 254 nm.

In the ICP-OES method, the sample after acid digestion is aspirated into the spray chamber, and from there to the torch, where an inductively coupled plasma provokes solvent evaporation and excitement of the analyte. The radiation emitted by the excited element is conducted by fiber optics or set of mirrors to a diffraction grating where it is decomposed into particular selected wavelengths and directed to the detector. The amount of radiation emitted by element is directly proportional to the amount of element present in the aspirated solution. The element concentration in the sample is determined by comparison with an analytical curve.

In the GFAAS, the sample is injected into a graphite tube and then through a drying step to remove the solvent. Subsequently, it is subjected to a pyrolysis step in the appropriate temperature for organic matter oxidation to complete mineralization and stabilization of the species of interest. This then forms an atomization precursor species of the analyte. The amount of radiant energy emitted by the lamp to a specific element of interest absorbed by the atomized analyte is proportional to the analyte concentration in the sample, which can be obtained by comparison with a calibration curve.

Sediment grain size determination

Sediment grain size determination was performed according to standard CETESB L6.160 [18]. This analysis is based on the principles of sieving and sedimentation guided by Wentworth scale, which is based on the average velocities of particles in an aqueous medium. According to this standard method, the sand fraction consists of particles with dimensions between 2.0 and 0.063 mm, coarse sand being comprised between the diameters from 1.0 to 2.0 mm. The silts are particles with the size between 0.063 and 0.004 mm, clays with a diameter smaller than 0.004 mm.

EF and I_{geo}

The Enrichment Factor (EF) is a factor that evaluate the enrichment of a given element through the normalization of another element considered stable and fixed in the environment and, then, compared to reference concentrations taking into account a normalizing element. This tool was proposed in 1979 by Buat-Menard [19–23] and has been applied in several regions of the world to evaluate anthropogenic enrichment of certain elements. The formula used for this calculation follows Eq. (1)

$$EF = (\mathrm{Me}/X)_{\mathrm{loc}} / (\mathrm{Me}/X)_{\mathrm{ref}} \quad (1)$$

where *EF* enrichment factor, *Me* metal or element analyzed, *X* metal or element normalize, *loc* study location, *ref* reference values.

Many elements can be used as normalizing elements, such as Sc, Fe, Al, Ti, Y and Li [10, 20, 24–26]. The present study used Sc as the normalizing element. As an enrichment evaluation criterion, some authors accept values between $0{,}5 \leq \mathrm{EF} \leq 1.5$ as indicators to show that an element is not enriched while values ≥ 1.5 indicate element enrichment [27]. However, for Hernandez et al. [24], only when the $\mathrm{EF} > 2.0$ it can be considered of anthropogenic origin. Sutherland [10], after justifying the absence or lack of criteria to define a level of pollution for the EF, proposed five enrichment categories, namely: $\mathrm{EF} < 2$, depleted or low enrichment; $2 < \mathrm{EF} < 5$, moderate enrichment; $5 < \mathrm{EF} < 20$, significant enrichment; $20 < \mathrm{EF} < 40$, very high enrichment and $\mathrm{EF} > 40$, extremely high enrichment.

The Geoaccumulation Index (I_{geo}) is a geochemical tool used to evaluate the contamination of a given location. The I_{geo} can be applied to organic and inorganic substances to evaluate contamination by comparing values of samples of pre-industrial locations or locations with no impact of the substances of interest. This index has been used for, at least, 30 years and is calculated using Eq. (2).

$$I_{\mathrm{geo}} = \log_2(C_n / 1.5 \times B_n), \quad (2)$$

where *log2* base 2 logarithms, C_n element concentration at the evaluated location, B_n element concentration in the reference values used (background).

A factor of 1.5 for B_n, according to several authors [5, 6, 20–22, 26], is applied to correct small fluctuations of lithogenic origin or even minor anthropogenic influences, in relation to background values. As the same as to EF,

the B_n variable represents the reference values (background) that should be used to represent element basal concentration. The same considerations for EF are used for this calculation. Several authors use earth crust values and others even prefer local values, believing these could be more representative. The I_{geo} Index is associated with a qualitative pollution intensity scale, shown in Table 1.

Both geochemical tools (EF and I_{geo}) for metal contamination studies are widely used by various researchers, using different sources as background references.

Table 1 I_{geo} values and contamination intensity

I_{geo}	Intensity (sediment quality)
<0	Not contaminated
0–1	Not contaminated to moderately contaminated
1–2	Moderately contaminated
2–3	Moderately to highly contaminated
3–4	Highly contaminated
4–5	Highly to very highly contaminated
>5	Very highly contaminated

Results and discussion

Grain size analysis of the sediments

Table 2 shows the results for the grain size determination of the sediment slices. Particle size determination indicates that the sediment is, predominantly, silty-clayed throughout the profile and characterized by a constant input of fine-grained material.

^{210}Pb dating and sedimentation rates

Isotopic ages for the profile are presented in Fig. 2. The ^{210}Pb profile depicts a linear trend ($r = 0.969$) from level 0 cm (year 2011) to level 36 cm (year 1922), with a mean sedimentation rate of 0.40 cm y^{-1}. This ^{210}Pb profile can be divided into two trends: from level 0 cm (year 2011) to level 12 cm (year 1964), indicating an average accumulation rate of 0.26 cm y^{-1} and from level 12 cm to level 36 cm (year 1922), indicating an average accumulation rate of 0.57 cm y^{-1}. Lower rates were related to the period prior to the water dam, when the loading of the sediments was stabilized. Higher rates were related to rainy seasons and urban expansion in the areas surrounding the reservoir. The values obtained at the latest slice were considered the background of the reservoir. This slice corresponded to sediment age of the 1920s.

Table 2 Grain size results for the sediment slices

Depth (cm)	Sand (%)	Silt (%)	Clay (%)
0–5	1.1	50.0	48.9
5–10	1.0	50.2	48.8
10–15	0.9	54.4	44.7
15–20	1.3	44.5	54.2
20–25	2.5	46.7	50.8
25–30	0.8	66.2	33.0
30–35	2.3	63.4	34.3
35–40	3.6	50.4	46.0

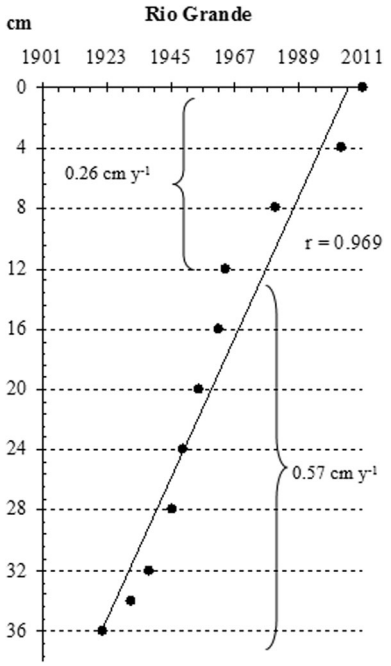

Fig. 2 ^{210}Pb profile and sedimentation rates

Inaa

The precision and accuracy of the INAA analytical methodology were verified by the analysis of reference materials and Z value calculation was done according to Bode [28]. If $|Z| < 3$, the individual result of the control sample (reference material) lies on the 99 % confidence interval of the target value. For the reference materials analyzed in the present study, all results were in the interval range of $|Z| < 3$, indicating good precision and accuracy of the INAA technique (Table 3). The z-value is calculated by using the Eq. (3):

$$Z_i = \frac{C_i - C_{\text{ref}}}{\sqrt{\sigma_i^2 + \sigma_{\text{ref}}^2}}, \quad (3)$$

where C_i: concentration of element i in the CRM analysis, C_{ref}: certified or consensus value of concentration for element i, σ_i: uncertainty of the element concentration i in the CRM analysis; σ_{ref}: uncertainty of the consensus value for element i.

Table 4 presents the results and respective uncertainties obtained by INAA. Tables 5 and 6 present EF and I_{geo} results, respectively. EF was calculated using Sc as the normalizing element; the results obtained for the last layer of the sampled profile (36–40 cm) were used as reference values (they were, also, used as reference values for I_{geo} calculations) and reflect the concentration of these elements during the 1920s (Fig. 2), when industrialization in the São Paulo Metropolitan Region was still incipient (Table 4).

EF results indicated that most of the elements did not present enrichment as I_{geo} results did for the elements As, Ba, Ca, Cr, Co, Cs, Fe, Sm, Eu, Lu, Rb, Th, Nd and Ta, which always showed values of $I_{\text{geo}} < 0.0$ and EF < 2.0, for the entire profile evaluated (Tables 4, 5). According to Sutherland [10], EF < 2.0 cannot be considered as anthropogenic enrichment. For this reason, Tables 4 and 5 only present results for the elements Ca, Ce, Co, Fe, Hf, La, Lu, Na, Sb, Sm, U, Yb and Zn for EF, while Ce, Na, Sb, U and Zn, for I_{geo}.

Although I_{geo} results of Ce and U showed no indication of accumulation, EF results pointed to a discreet enrichment in the middle of the profile (Ce—25–35 cm depth; U—25–30 cm depth) (Figs. 3). This could be related to sources of pollution which existed in the past, but, today they either do not exist any longer, or they are under control. Figure 3 shows the behavior of these two elements along the profile.

Regarding the elements Na, Sb and Zn, EF results (>2.0), at the top of the profile, pointed to an enrichment, which can be considered as anthropogenic origin,

Table 3 Z-score values obtained for the elements analyzed by INAA

	Soil 5			BEN basalt			SL1		
	Obtained values	Certified values	Z score	Obtained values	Certified values	Z score	Obtained values	95 % Conf. interval	Z score
As	91.6 ± 10.1	93.9 ± 7.5	−0.18	*nd*	1.8 ± 0.3		28.3 ± 2.4	24.7–30.5	−0.32
Ba	554 ± 46	561 ± 53	−0.10	1123 ± 99	1025 ± 30	0.94	592 ± 49	586–692	−0.64
Ca (%)	2.75 ± 0.10	(2.2)	2.20	83.1 ± 2.6	99.1 ± 2.2	−2.60	*nd*		
Ce	58 ± 5	57.9 ± 3.0	0.07	174 ± 14	152 ± 12	1.50	105 ± 3	100–134	−0.71
Co	15.4 ± 0.5	14.8 ± 0.76	0.48	60.8 ± 2.0	60 ± 2	0.33	18.8 ± 0.4	18.3–21.3	−0.61
Cr	26.2 ± 1.5	28.9 ± 2.8	−0.85	366 ± 25	360 ± 12	0.20	113 ± 7	95–113	0.82
Cs	74.8 ± 15.2	56,7 ± 6.6	1.17	0.62 ± 0.15	0.8 ± 0.1	−0.49	7.1 ± 1.5	6.1–7.9	0.04
Eu	1.14 ± 0.13	1.18 ± 0.08	0.36	3.55 ± 0.39	3.6 ± 0.18	−0.47	1.70 ± 0.06	1.1–2.1	0.06
Fe (%)	4.76 ± 0.09	4.45 ± 0.19	1.45	8.95 ± 0.16	8.98 ± 0.08	−0.04	6.32 ± 0.10	6.57–6.91	−1.82
Hf	6.01 ± 0.33	6.30 ± 0.30	−0.64	5.83 ± 0.32	5.6 ± 0.16	0.40	4.24 ± 0.11	3.6–4.8	0.40
La	29.0 ± 0.7	28.1 ± 1.5	0.29	86.2 ± 2.5	82 ± 1.5	1.14	48.6 ± 1.0	49.5–55.7	−1.02
Lu	0.38 ± 0.05	0.336 ± 0.044	0.62	0.24 ± 0.04	0.24 ± 0.03	−0.06	0.48 ± 0.05	0.41–0.67	−0.64
Na	19787 ± 750	*	*	23916 ± 1124	23600 ± 400	0.27	1628 ± 69	1600–1800	−0.59
Nd	24 ± 4	29.9 ± 1.6	−1.28	83 ± 14	67 ± 1.5	1.07	59 ± 6	*	*
Rb	130 ± 10	138 ± 7.4	−0.55	50.2 ± 4.9	47 ± 2	0.61	112 ± 8.0	102–124	−0.09
Sb	12.7 ± 1.2	14.3 ± 2.2	−1.24	*nd*	0.26 ± 0.05		0.73 ± 0.10	1.19–1.43	−2.02
Sc	15.8 ± 0.7	14.8 ± 0.66	0.97	22.6 ± 0.9	22 ± 0.15	0.33	15.8 ± 0.65	16.2–18.4	−1.12
Sm	5.93 ± 0.19	5.42 ± 0.39	1.17	11.5 ± 0.5	12.2 ± 0.3	−1.22	9.03 ± 0.34	8.74–9.76	−0.37
Ta	0.65 ± 0.12	0.764 ± 0.056	0.36	9.1 ± 1.5	5.7 ± 0.4	1.90	1.32 ± 0.17	1.00–2.16	−0.74
Th	11.0 ± 0.5	11.3 ± 0.7	−0.32	11.0 ± 0.6	10.4 ± 0.65	0.75	13.5 ± 0.63	13–15	−0.39
U	3.38 ± 0.32	3.04 ± 0.51	−0.24	2.45 ± 0.28	2.4 ± 0.18	0.60	3.63 ± 0.38	3.69–4.35	−0.40
Yb	2.39 ± 0.24	2.24 ± 0.20	0.12	1.90 ± 0.18	1.8 ± 0.2	−0.42	3.16 ± 0.25	2.77–4.07	0.25
Zn	390 ± 24	368 ± 8	0.87	131 ± 5	120 ± 13	0.81	193 ± 12	213–233	−1.93

nd Not determined

* Not informed

Table 4 Results for the sediment samples by INAA along the profile (mg kg^{-1}), dating of the sediment slices and the upper continental crust (UCC) values [27]

Depth	Year	As	Ba	Ca (%)	Ce	Co	Cr	Cs	Eu	Fe (%)	Hf	La	Lu
0–2	2011–2004	26 ± 3	522 ± 34	1.10 ± 0.04	97 ± 6	12.2 ± 0.3	82 ± 4	5.2 ± 0.5	0.75 ± 0.06	9.74 ± 0.12	5.0 ± 0.2	41.3 ± 0.8	0.37 ± 0.04
2–4	2004–1996	28 ± 3	500 ± 33	1.14 ± 0.04	98 ± 6	11.5 ± 0.3	88 ± 4	5.7 ± 0.5	0.69 ± 0.07	9.16 ± 0.11	5.4 ± 0.2	39.7 ± 0.8	0.43 ± 0.04
4–6	1996–1988	25 ± 3	541 ± 34	1.29 ± 0.04	92 ± 5	10.6 ± 0.3	92 ± 4	5.3 ± 0.5	0.80 ± 0.05	8.61 ± 0.11	5.2 ± 0.2	37.0 ± 0.7	0.37 ± 0.04
6–8	1988–1980	28 ± 3	478 ± 32	1.19 ± 0.04	94 ± 5	10.4 ± 0.3	92 ± 4	6.0 ± 0.6	0.77 ± 0.05	8.69 ± 0.11	4.8 ± 0.2	37.9 ± 0.7	0.35 ± 0.04
8–10	1980–1972	31 ± 4	562 ± 36	0.95 ± 0.04	92 ± 5	9.9 ± 0.2	96 ± 4	6.3 ± 0.6	0.67 ± 0.06	8.34 ± 0.10	4.8 ± 0.2	40.1 ± 0.8	0.36 ± 0.04
10–12	1972–1964	27 ± 3	464 ± 31	0.97 ± 0.04	90 ± 5	8.7 ± 0.2	94 ± 4	5.9 ± 0.6	0.70 ± 0.05	8.00 ± 0.10	5.1 ± 0.2	34.2 ± 0.7	0.35 ± 0.03
14–16	1964–1961	23 ± 3	487 ± 32	1.15 ± 0.04	92 ± 5	7.8 ± 0.2	98 ± 5	6.0 ± 0.6	0.74 ± 0.08	7.16 ± 0.09	5.2 ± 0.2	35.4 ± 0.7	0.41 ± 0.04
16–18	1961–1958	27 ± 2	579 ± 43	1.28 ± 0.04	101 ± 6	8.6 ± 0.2	121 ± 6	6.3 ± 0.5	0.84 ± 0.09	7.51 ± 0.09	5.9 ± 0.3	27.4 ± 0.6	0.33 ± 0.03
18–20	1958–1954	24 ± 2	501 ± 40	1.25 ± 0.04	110 ± 6	9.1 ± 0.2	113 ± 5	5.9 ± 0.5	0.77 ± 0.06	7.55 ± 0.09	5.6 ± 0.2	30.5 ± 0.6	0.40 ± 0.04
20–22	1954–1951	30 ± 2	490 ± 37	1.19 ± 0.04	114 ± 6	8.6 ± 0.2	115 ± 6	6.1 ± 0.9	0.85 ± 0.09	7.89 ± 0.10	5.9 ± 0.3	33.5 ± 0.7	0.40 ± 0.04
22–24	1951–1947	28 ± 2	536 ± 40	1.03 ± 0.04	109 ± 6	10.5 ± 0.3	104 ± 5	6.3 ± 0.9	0.85 ± 0.09	8.48 ± 0.10	6.3 ± 0.2	31.3 ± 0.6	0.40 ± 0.04
24–26	1947–1944	25 ± 2	467 ± 38	1.04 ± 0.04	109 ± 6	9.8 ± 0.2	91 ± 4	6.1 ± 0.5	0.73 ± 0.07	7.84 ± 0.10	6.2 ± 0.2	26.1 ± 0.5	0.46 ± 0.05
26–28	1944–1940	26 ± 2	525 ± 42	1.12 ± 0.04	135 ± 8	9.3 ± 0.2	80 ± 4	5.1 ± 0.4	0.68 ± 0.04	7.42 ± 0.09	5.9 ± 0.2	22.9 ± 0.5	0.45 ± 0.05
28–30	1940–1937	28 ± 2	571 ± 45	1,02 ± 0,03	158 ± 9	9.6 ± 0.2	85 ± 4	7.8 ± 0.4	0.75 ± 0.06	7.05 ± 0.06	6.0 ± 0.2	29.0 ± 0.6	0.48 ± 0.05
30–32	1937–1933	31 ± 2	592 ± 44	1.00 ± 0.04	162 ± 9	9.8 ± 0.2	82 ± 4	4.7 ± 0.7	0.80 ± 0.06	7.26 ± 0.09	6.1 ± 0.2	33.3 ± 0.7	0.44 ± 0.05
32–34	1933–1930	28 ± 2	542 ± 33	1.13 ± 0.04	146 ± 8	11.2 ± 0.3	83 ± 4	5.4 ± 0.4	0.83 ± 0.05	7.52 ± 0.09	7.1 ± 0.3	29.6 ± 0.6	0.48 ± 0.05
34–36	1930–1926	29 ± 2	523 ± 32	1.09 ± 0.04	123 ± 6	11.6 ± 0.3	83 ± 4	5.8 ± 0.5	0.77 ± 0.05	7.71 ± 0.09	7.9 ± 0.3	25.5 ± 0.5	0.52 ± 0.05
36–40	1926–1922	27 ± 2	550 ± 44	1.57 ± 0.04	83.0 ± 5	9.4 ± 0.2	91 ± 4	5.8 ± 0.5	0.66 ± 0.05	7.00 ± 0.08	7.2 ± 0.3	31.5 ± 0.6	0.53 ± 0.06
UCC		2.0	668	2.95	65	11.6	35	5.8	0.95	3.09	5.8	32.3	0.27

Depth	Year	Na	Nd	Rb	Sb	Sc	Sm	Ta	Th	U	Yb	Zn
0–2	2011–2004	4490 ± 166	20 ± 3	79 ± 5	2.3 ± 0.2	17.9 ± 0.6	4.5 ± 0.2	1.5 ± 0.1	18.1 ± 0.7	5.0 ± 0.5	1.6 ± 0.1	164 ± 8
2–4	2004–1996	3854 ± 135	25 ± 3	96 ± 6	2.5 ± 0.3	19.2 ± 0.7	5.2 ± 0.2	1.5 ± 0.3	20.0 ± 0.8	4.8 ± 0.6	2.1 ± 0.2	146 ± 7
4–6	1996–1988	3422 ± 126	16 ± 3	89 ± 5	2.6 ± 0.3	19.1 ± 0.7	4.2 ± 0.1	1.7 ± 0.1	19.7 ± 0.8	5.1 ± 0.5	1.9 ± 0.2	134 ± 7
6–8	1988–1980	3126 ± 132	18 ± 3	89 ± 5	2.6 ± 0.3	19.8 ± 0.7	5.0 ± 0.2	1.8 ± 0.1	19.5 ± 0.8	5.1 ± 0.5	1.6 ± 0.1	123 ± 6
8–10	1980–1972	3113 ± 204	18 ± 2	94 ± 6	2.9 ± 0.3	19.8 ± 0.7	4.6 ± 0.2	1.7 ± 0.1	19.7 ± 0.8	5.3 ± 0.5	1.7 ± 0.1	119 ± 6
10–12	1972–1964	1490 ± 166	21 ± 2	88 ± 5	2.4 ± 0.2	20.4 ± 0.7	4.7 ± 0.2	1.8 ± 0.2	20.5 ± 0.8	3.5 ± 0.3	1.9 ± 0.2	120 ± 6
14–16	1964–1961	2624 ± 111	25 ± 2	95 ± 5	1.7 ± 0.2	20.1 ± 0.7	4.5 ± 0.2	1.7 ± 0.1	19.9 ± 0.8	5.1 ± 0.6	2.0 ± 0.1	113 ± 6
16–18	1961–1958	1033 ± 35	15 ± 2	93 ± 6	1.9 ± 0.2	20.0 ± 0.7	3.6 ± 0.1	1.8 ± 0.1	21.1 ± 0.8	5.4 ± 0.5	2.1 ± 0.2	123 ± 6
18–20	1958–1954	1080 ± 34	17 ± 2	109 ± 9	1.4 ± 0.1	20.5 ± 0.7	4.6 ± 0.1	1.9 ± 0.1	20.9 ± 0.8	6.1 ± 0.5	1.8 ± 0.1	149 ± 9
20–22	1954–1951	964 ± 34	25 ± 4	91 ± 6	1.5 ± 0.1	19.7 ± 0.7	3.9 ± 0.1	1.9 ± 0.1	21.6 ± 0.8	5.8 ± 0.4	2.4 ± 0.2	124 ± 6
22–24	1951–1947	978 ± 38	16 ± 3	87 ± 6	1.5 ± 0.1	19.8 ± 0.7	3.6 ± 0.1	1.9 ± 0.1	21.6 ± 0.9	5.1 ± 0.5	2.4 ± 0.2	131 ± 6
24–26	1947–1944	890 ± 29	20 ± 2	104 ± 8	1.2 ± 0.1	20.2 ± 0.7	3.9 ± 0.1	2.0 ± 0.2	21.3 ± 0.8	6.3 ± 0.7	2.4 ± 0.2	156 ± 9
26–28	1944–1940	896 ± 30	14 ± 1	134 ± 10	0.8 ± 0.2	22.1 ± 0.8	3.3 ± 0.1	1.8 ± 0.1	22.4 ± 0.9	6.9 ± 0.8	2.5 ± 0.2	104 ± 6
28–30	1940–1937	824 ± 28	23 ± 5	130 ± 8	0.53 ± 0.05	21.7 ± 0.8	3.8 ± 0.1	2.4 ± 0.3	22.8 ± 0.9	8.4 ± 0.6	2.6 ± 0.2	87 ± 4

Table 4 continued

Depth	Year	Na	Nd	Rb	Sb	Sc	Sm	Ta	Th	U	Yb	Zn
30–32	1937–1933	581 ± 32	16 ± 2	135 ± 8	0.74 ± 0.05	21.5 ± 0.8	3.3 ± 0.1	1.8 ± 0.1	22.9 ± 0.9	7.6 ± 0.6	2.9 ± 0.2	70 ± 4
32–34	1933–1930	705 ± 25	20 ± 2	133 ± 10	0.70 ± 0.07	21.4 ± 0.7	3.4 ± 0.1	1.9 ± 0.1	24.2 ± 0.9	7.3 ± 0.8	3.1 ± 0.2	90 ± 6
34–36	1930–1926	938 ± 32	21 ± 3	117 ± 9	1.1 ± 0.1	20.9 ± 0.7	3.7 ± 0.1	2.1 ± 0.2	24.0 ± 0.9	5.0 ± 0.4	3.0 ± 0.2	95 ± 7
36–40	1926–1922	1048 ± 34	23 ± 4	96 ± 7	1.1 ± 0.1	21.1 ± 0.7	3.6 ± 0.1	2.1 ± 0.1	22.8 ± 0.9	4.8 ± 0.3	2.8 ± 0.2	77 ± 4
UCC		25670	25.9	110	0.31	7	4.7	1.5	10.3	2.5	1.5	52

according to Sutherland [10] or Zhang & Liu [26] classification. The I_{geo} for these elements, also, presented values greater than zero. The concentrations for Na at the top of the profile were considered moderately enriched by both criteria ($3.0 < EF < 5.0$ and $I_{geo} > 1.0$), while $2.0 < EF < 3.0$ and $0 < I_{geo} < 1.0$, for Sb and Zn, were considered a light to moderate enrichment (Table 6).

It should be noted that the values obtained in this study for various elements, most notably As, Cr, Ce, Fe, Zn, Sb, Th, Sc and U, presented concentrations at the base of the profile (and in some cases throughout the entire profile) well above those set by Wedepohl [27] as Upper Continental Crust values. Concentrations obtained for Ba, Ca and Na at the reservoir were smaller than those established by Wedepohl [27] (Table 4).

It becomes clear that, in this case, the use of local geochemical values for anthropogenic enrichment or contamination assessment is crucial for correct environmental evaluations. If, in this study, the values set by Wedepohl [27] had been taken as reference values, the conclusions would have been very different. For example, As that presented a concentration between 23.4 and 31.2 mg kg^{-1} throughout the entire profile would have been considered highly contaminated, with an $I_{geo} > 3.0$ and an $EF > 12.0$, compared to the defined value for As in the continental crust of 2.0 mg kg^{-1}. In this study, the $EF < 1.5$ and $I_{geo} < 0$ were obtained for As using the concentration of the base of the profile as reference value.

As mentioned before, other studies [8, 11, 29] developed at this reservoir for the purpose of metal concentration evaluation have already been published. The concentration values obtained by these authors for REE and As, Ba, Co, Fe, Rb, Sb and Zn were very similar to the present study. These studies, also, concluded that the sediments from this reservoir, collected in points near the point of this study, could be contaminated with some elements such as As, Cs, Sb, Lu, Yb, Th, Hf and U due to the values obtained for the Enrichment Factors ($EF > 2.0$), using the earth crust as reference values [27]. From these data, it was possible to conclude that the choice of the background geochemical values is fundamental, not only for the correct interpretation of the geochemical data, but, as well as for the anthropogenic contamination evaluation. In the case of anthropogenic contamination evaluation of sediments, the utilization of a sedimentary profile may offer an adequate answer to this question.

Metal determination by ICP-OES, GFAAS and direct mercury analyzer (DMA)

The certified reference materials analyses of RTC CRM049-050 (Sandy Clay), NIST SRM 8704 (Buffalo

Table 5 Enrichment factor (EF) results (only elements that showed EF > 0.5 along the profile)

Depth	Ca	Ce	Co	Fe	Hf	La	Lu	Na	Sb	Sm	U	Yb	Zn
0–2	0.8	1.4	1.5	1.6	0.8	1.5	0.8	5.0	2.6	1.5	1.2	0.7	2.5
2–4	0.8	1.3	1.3	1.4	0.8	1.4	0.9	4.0	2.5	1.6	1.1	0.8	2.1
4–6	0.9	1.2	1.2	1.4	0.8	1.3	0.8	3.6	2.7	1.3	1.2	0.7	1.9
6–8	0.8	1.2	1.2	1.3	0.7	1.3	0.7	3.2	2.6	1.5	1.1	0.6	1.7
8–10	0.6	1.2	1.1	1.3	0.7	1.4	0.7	3.2	2.9	1.4	1.2	0.7	1.6
10–12	0.6	1.1	1.0	1.2	0.7	1.1	0.7	1.5	2.3	1.3	0.7	0.7	1.6
14–16	0.8	1.2	0.9	1.1	0.8	1.2	0.8	2.6	1.6	1.3	1.1	0.8	1.5
16–18	0.9	1.3	1.0	1.1	0.9	0.9	0.7	1.0	1.9	1.0	1.2	0.8	1.7
18–20	0.8	1.4	1.0	1.1	0.8	1.0	0.8	1.1	1.4	1.3	1.3	0.7	2.0
20–22	0.8	1.5	1.0	1.2	0.9	1.1	0.8	1.0	1.5	1.2	1.3	0.9	1.7
22–24	0.7	1.4	1.2	1.3	0.9	1.1	0.8	1.0	1.5	1.1	1.1	0.9	1.8
24–26	0.7	1.4	1.1	1.2	0.9	0.9	0.9	0.9	1.2	1.1	1.4	0.9	2.1
26–28	0.7	1.6	0.9	1.0	0.8	0.7	0.8	0.8	0.7	0.9	1.4	0.8	1.3
28–30	0.6	1.8	1.0	1.0	0.8	0.9	0.9	0.8	0.5	1.0	1.7	0.9	1.1
30–32	0.6	1.9	1.0	1.0	0.8	1.0	0.8	0.5	0.7	0.9	1.6	1.0	0.9
32–34	0.7	1.7	1.2	1.1	1.0	0.9	0.9	0.7	0.6	0.9	1.5	1.1	1.2
34–36	0.7	1.5	1.2	1.1	1.1	0.8	1.0	0.9	1.0	1.0	1.0	1.1	1.2
36–40	1.0	1.0	1.0	1.0	1.0	1.0	1.0	1.0	1.0	1.0	1.0	1.0	1.0

Table 6 Geoaccumulation index (I_{geo}) results

Depth	Ce	Na	Sb	U	Zn
0–2	<0	1.5	0.5	<0	0.5
2–4	<0	1.3	0.6	<0	0.3
4–6	<0	1.1	0.7	<0	0.2
6–8	<0	1.0	0.7	<0	0.1
8–10	<0	1.0	0.8	<0	0.0
10–12	<0	<0	0.6	<0	0.1
14–16	<0	0.7	0.1	<0	<0
16–18	<0	<0	0.2	<0	0.1
18–20	<0	<0	<0	<0	0.4
20–22	<0	<0	<0	<0	0.1
22–24	<0	<0	<0	<0	0.2
24–26	<0	<0	<0	<0	0.4
26–28	0.1	<0	<0	<0	<0
28–30	0.3	<0	<0	0.2	<0
30–32	0.4	<0	<0	0.1	<0
32–34	0.2	<0	<0	0.1	<0
34–36	<0	<0	<0	<0	<0
36–40	<0	<0	<0	<0	<0

River Sediment), and NIST SRM 2710 (Montana Soil) were carried out under the same conditions of the samples: the results obtained are shown in Table 7. The *Z*-score was calculated for all results and were in the range of interval $|Z| < 3$, indicating good precision and accuracy for all analytical methodologies applied. The results obtained (mean of replicates ± uncertainty) may be seen in Table 8. The incertainty was calculated according to Franklin et al. [29].

Tables 9 and 10 show the enrichment factor and I_{geo} for the elements analyzed, respectively.

It is clear that the great enrichment (EF) for Cd and Cu in the top of the profile, with values of 26.9 and 232, respectively, confirmed by I_{geo} of 4.1 and 7.2, respectively, indicates extremely contaminated sediment (Tables 9, 10). Such surface contamination for these elements indicates that the probable sources may still be active in the reservoir and may still be releasing these elements. In the case of Cu, this may be due to the use of its salts, mainly $CuSO_4$, applied by the company responsible for the water treatment to prevent algae growth in the reservoir. In relation to Cd, there is no knowledge about pollution sources in the reservoir. Regarding Ni and Mn, a moderate enrichment more significant on the surface of the profile could be observed. This moderate contamination was, also, confirmed by I_{geo}, with values between 0 and 1 for Ni and 1.1 and 1.7 for Mn (Table 10). In relation to Hg and Pb enrichment, it is more significant in the middle of the profile, indicating that in the past there was a strong anthropogenic contribution of these elements, especially for Hg (EF from 91 to 128 and I_{geo} from 5.7 to 6.4). The current depletion of

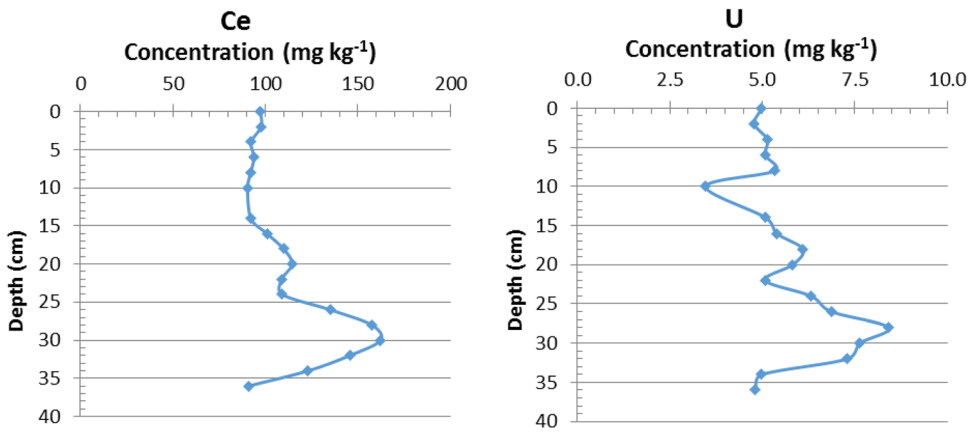

Fig. 3 Behavior of Ce and U along the sediment core

Table 7 Results of the Certified Reference Materials analyzes by ICP-OES, GF AAS and DMA (mg kg^{-1})

	Mn	Ni	Cu	Cd	Pb	Hg
Certified values						
CRM049-050	636 ± 21	344 ± 6	88.5 ± 1.7	80.0 ± 1.3	111 ± 2	13.5 ± 0.4
SRM 8704	544 ± 21	42.9 ± 3.7	–	2.94 ± 0.29	150 ± 17	–
SRM 2710	2140 ± 60	8 ± 1	3420 ± 50	12.3 ± 0.3	5520 ± 30	9.88 ± 0.21
Obtained values						
CRM049-050	593 ± 25	340 ± 9	89.1 ± 2.0	76.7 ± 2.2	110 ± 5	12.9 ± 1.1
SRM 8704	479 ± 12	37.6 ± 1.4	–	3.45 ± 0.19	140 ± 6	–
SRM 2710	1963 ± 80	7.21 ± 0.29	3355 ± 22	13.88 ± 0.57	–	9.52 ± 0.44
Z score						
CRM049-050	−1.32	−0.37	0.24	−1.29	−0.18	−0.51
SRM 8704	−2.69	−1.34	–	1.47	−0.55	–
SRM 2710	−1.77	−0.76	−1.19	2.45	–	−0.74

Table 8 Results obtained for elements determined by ICP-OES, GF AAS and DMA (mg kg^{-1})

Depth (cm)	Pb[a]	Hg[b]	Cd[a]	Cu[c]	Ni[c]	Mn[c]
0–5	52.9 ± 2.5	0.55 ± 0.08	1.02 ± 0.06	4867 ± 54	25.2 ± 2.1	907 ± 28
5–10	57.0 ± 2.4	0.68 ± 0.05	0.90 ± 0.07	5404 ± 62	26.4 ± 2.0	810 ± 21
10–15	69.7 ± 2.7	1.3 ± 0.1	0.69 ± 0.05	3774 ± 48	30.4 ± 2.1	599 ± 19
15–20	72.6 ± 2.9	2.7 ± 0.2	0.45 ± 0.03	1112 ± 27	33.9 ± 2.0	585 ± 22
20–25	60.0 ± 2.5	17.3 ± 1.1	0.30 ± 0.03	244 ± 10	22.9 ± 1.8	475 ± 16
25–30	42.4 ± 2.4	10.7 ± 0.9	0.06 ± 0.01	36.4 ± 1.9	14.9 ± 1.8	290 ± 13
30–35	38.6 ± 2.3	0.58 ± 0.06	0.05 ± 0.01	25.9 ± 1.1	13.3 ± 1.5	375 ± 15
35–40	29.0 ± 2.1	0.14 ± 0.03	0.04 ± 0.01	22.1 ± 1.0	10.9 ± 1.5	181 ± 12

[a] GF AAS

[b] DMA

[c] ICP OES

Table 9 EF values obtained from the metals results

Enrichment factor (EF)						
Depth (cm)	Pb	Hg	Cd	Cu	Ni	Mn
0–5	1.9	4.1	26.9	232	2.4	5.3
5–10	1.9	4.7	22.0	239	2.4	4.4
10–15	2.1	7.9	14.7	146	2.4	2.8
15–20	2.5	19.0	11.1	49.8	3.1	3.2
20–25	2.2	128	7.8	11.5	2.2	2.7
25–30	1.7	90.8	1.8	2.0	1.6	1.9
30–35	1.6	5.0	1.5	1.4	1.5	2.5
35–40	1.0	1.0	1.0	1.0	1.0	1.0

Table 10 I_{geo} values obtained from the metals results

Geoaccumulation index						
Depth (cm)	Pb	Hg	Cd	Cu	Ni	Mn
0–5	0.3	1.4	4.1	7.2	0.6	1.7
5–10	0.4	1.7	3.9	7.3	0.7	1.6
10–15	0.7	2.6	3.5	6.8	0.9	1.1
15–20	0.7	3.7	2.9	5.1	1.1	1.1
20–25	0.5	6.4	2.3	2.9	0.5	0.8
25–30	0.0	5.7	0.0	0.1	<0	0.1
30–35	<0	1.5	<0	<0	<0	0.5
35–40	<0	<0	<0	<0	<0	<0

these concentrations on the surface is an indication that these sources are controlled or no longer exist. Figure 4 shows the behavior of Cd, Hg and Pb along the sediment profile.

Fávaro et al. [11] determined the multielemental concentrations of sediment cores from Rio Grande Reservoir by INAA, Hg content by CVAAS and sedimentation rates by ^{210}Pb method. For the sediment core located near the entrance of the reservoir (opposite location of the sediment profile collected in the present study), a peak of 11,586 mg Hg kg^{-1} was found in 1949 and at the end of the core (1932), values about 0.145 mg Hg kg^{-1} were found. The authors concluded that this core showed a strong anthropogenic influence in the Hg concentration probably due to the discharges from the chloralkali industry, located near this core. This industry has been operating at the Rio Grande Reservoir since 1948. The influence is also apparent in the others cores analyzed located downstream. In the present study, a peak in the Hg content of 17.3 mg kg^{-1} was found around the 1950s (Fig. 4) decreasing to 0.14 mg kg^{-1} at the 35–40 cm depth (approximately 1920). The results obtained for Hg were very similar in both studies.

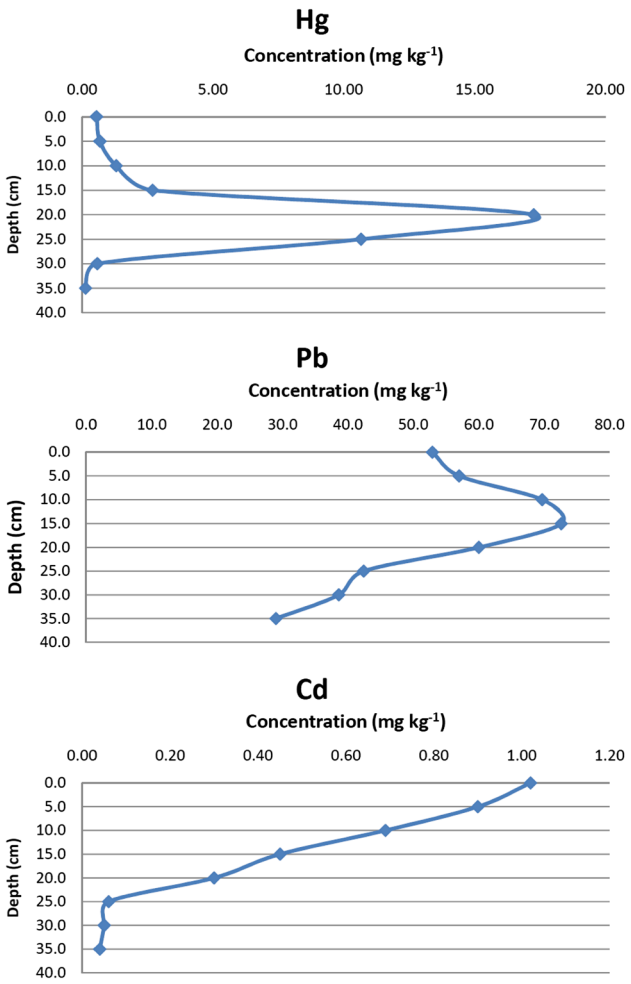

Fig. 4 Behavior of Pb, Hg and Cd along the sediment core

Conclusion

The ^{210}Pb profile showed an average accumulation rate of 0.26 cm y^{-1} in the upper segments of the sediment profile (2011–1964 year) and average accumulation rate of 0.57 cm y^{-1} (1964–1922 year) in the lower section, clearly reflecting the different periods of sediment loading in this reservoir.

The Enrichment Factor and Geoaccumulation Index are excellent tools for environmental evaluations and in this study they presented results aligned with the anthropogenic enrichment of some analyzed elements.

Most of the elements presented concentrations very similar in this reservoir, along the time. Cu and Cd have severe anthropogenic contributions in the reservoir, the same occurring for Hg. But, for this element, a peak in the concentration in the middle of the profile was observed, indicating that there was a source in the past that nowadays appears to be under control: nevertheless, the concentration in the surface is still considered high (0.55 mg kg^{-1}). In

the case of Cu, the use of $CuSO_4$ by the company responsible for water treatment to prevent algae growth in the reservoir is probably the cause of the contamination. In relation to Cd, there is not any knowledge about pollution sources in the reservoir. However, a discreet anthropogenic enrichment for Ni, Pb and Sb and a moderate enrichment for Na and Mn are observed. In general, all other elements and rare earth elements presented constant values throughout the sediment profile.

For this study, background values for metals and trace elements in the sediments from the Rio Grande Reservoir were considered as the concentration present in the lowest slice of the profile, corresponding to the date of 1920. At that time, the industrialization of São Paulo was nearly non-existent and in its very early development stages. As for the data of this study, it can be observed that the choice of the local geochemical background values are fundamental for the correct interpretation of the anthropogenic contamination of sediments evaluation.

References

1. CETESB (2011) Qualidade das águas superficiais no estado de São Paulo—(2010)—Apêndice B. CETESB, São Paulo
2. Cánovas CR, Olias M, Vasquez-Suné E, Ayora C, Nieto JM (2012) Sci Tot Environ 416:418–428
3. Silvério PF (2003) Bases técnico-científicas para derivação de valores guia de qualidade de sedimentos para metais: experimentos de campo e laboratório. PhD Thesis, Escola de Engenharia de São Carlos-USP, p 145
4. Quináglia GA (2012) Caracterização dos Níveis basais de Concentração de metais nos sedimentos do sistema estuarino da Baixada Santista. Biblioteca 24 horas, São Paulo
5. Gomes FC, Godoy JM, Godoy MLDP, Carvalho ZL, Lopes RT, Sanchez-Cabeza JAS, Lacerda LD, Wasserman JL (2009) Mar Poll Bull 59:123–133
6. Audry S, Schaefer J, Blanc G, Jousnneau J-M (2004) Environ Pollut 132(3):413–426
7. Albarede F (2011) Geoquímica. Uma Introdução. Oficina de Textos, São Paulo
8. Franklin RL, Ferreira FJ, Bevilacqua JE, Fávaro DIT (2012) J Radioanal Nucl Chem 291(1):147–153
9. Luiz-Silva W, Machado W, Matos RHR (2008) J Braz Chem Soc 19(8):1490–1500
10. Sutherland RA (2000) Environ Geol 39(6):611–627
11. Fávaro DIT, Damatto SR, Moreira EG, Mazzilli BP, Campagnoli F (2007) J Radioanal Nucl Chem 273(2):451–463
12. Bostelman E, (2006) Avaliação da concentração de metais em amostras de sedimento do reservatório Billings, braço Rio Grande, São Paulo, Brasil. MSc Thesis, IPEN-USP, p 117
13. Moreira EG, Vasconcellos MBA, Saiki M (2006) J Radioanal Nucl Chem 269(2):377–382
14. Larizatti FE, Fávaro DIT, Moreira SRD, Mazzilli BP, Piovano EL (2001) J Radioanal Nucl Chem 249(1):263–268
15. Damatto SR (2009) In: Proceedings of international tropical conference on Po and radioactive Pb isotopes, Sevilla, España
16. Leonardo L, Damatto SR, Gios BR, Mazzilli BP (2014) J Radioanal Nucl Chem 299(3):1935–1941
17. http://www.epa.gov/epawaste/hazard/testmethods/sw846/pdfs/3051a.pdf. Accessed 23 Jan 2012
18. Norma técnica L6.160 (1995) Sedimentos: determinação da distribuição granulométrica-método de ensaio. CETESB, São Paulo
19. Loska K, Cebula J, Pelczar J, Wiechula D (1997) Kwapuliski. Water Air Soil Poll 93:347–365
20. Loska K, Wiechula D, Barska B, Cebula E, Chojnecka A (2003) Poll J Environ Stud 12(2):187–193
21. Loska K, Wiechula D, Korus I (2004) Environ Inter 30:159–163
22. Szefer P, Skwarzec B (1988) Mar Chem 23:109–129
23. Dias MI, Prudencio MI (2008) Microchem J 88:136–141
24. Hernandez L, Probst A, Probst JL, Ulrich E (2003) Sci Tot Environ 312:195–219
25. Lin C, He M, Zhou Y, Guo W, Yang Z (2008) Environ Monit Assess 137:329–342
26. Zhang J, Liu CL (2002) Est Coast Shelf Sci 54:1051–1070
27. Wedepohl KH (1995) Geochim Cosmochim Act 59(7):1217–1232
28. Bode P (1996) Instrumental and organizational aspects of a neutron activation analysis laboratory. Interfaculty Reactor Institut, Delft
29. Franklin RL, Bevilacqua JE, Fávaro DIT (2012) Quím Nova 35(1):45–50